A HIGH-RESOLUTION ANALYSIS METHOD OF INSTABILITY ENERGY

Li Hongji (李洪勣), *Xu Hong* (徐 宏) and *Wang Ronghua* (王荣华)

Air Force Meteorological Research Institute

Received August 11, 1986

ABSTRACT

This paper describes a geopotential thickness difference method for computing instability energy E. $E_{P_1}^{P_2}=g_c\left(\Delta H_s{}_{P_1}^{P_2}-\Delta H_{P_1}^{P_2}\right)$, where $\Delta H_{P_1}^{P_2}$ is the geopotential thickness of P_1-P_2 level; $\Delta H_s{}_{P_1}^{P_2}$ is called adiabatic geopotential thickness, based on which a computational method for high resolution of instability energy is proposed. $E(x,y)\approx g_0(A(x,y)-B(x,y))$, where A is interpolating polynomial of $\Delta H_s{}_{P_1}^{P_2}$ and it is a function of θ_e of surface observing stations (x,y); $B(x,y)$ is the thickness over corresponding stations (x, y) obtained using surface fitting method. Therefore, data of METAR can be used by computer to produce hourly horizontal distribution chart of E of surface observing station density. With the result that the temporal and spatial resolution of stability analysis has been improved. Practical use has shown that this method is an effective tool for very short range forecast of severe convective storms.

1. INTRODUCTION

The application of computers and advanced communication equipment to very short range weather forecast in recent years has improved the ability of monitoring and very short range forecast of severe convective storms. It is of importance to further improve the effectiveness of very short range forecast and to study and use better methods for analyses and forecasts. In the atmosphere, motion systems of certain size are primarily due to certain types of force within the equations of motion. For the occurrence of severe convective storms, buoyancy is primary. Though a part of kinetic energy can be obtained from ambient wind field during its development process, actually instability energy release is the main source of energy required by its development (Chao Jiping and Zhou Xiaoping, 1964). In atmospheric thermodynamics, an adiabatic ascending parcel gains energy or instability energy E when it passes through pressure levels p_1-p_2 because of net buoyancy.

$$E_{P_1}^{P_2}=-R_d\int_{p_1}^{p_2}(T_{vi}-T_{ve})d\ln p \qquad (1)$$

where R_d is the gas constant of dry air; T_{vi} and T_{ve} are the virtual temperature of parcel and ambient air, respectively. Computation of instability energy E from equation (1) requires complete sounding curves. Because it is inconvenient to use Eq. (1), E is seldom computed in operational work. Therefore, some stability indices are often used. By using 620 days of sounding data at 0800 in July and August from 1969 to 1978 in Beijing, we have computed E and various stability factors and compared their efficiencies in forecasting thunderstorms.

When the ratio of missing is taken as 1/5, statistics of accuracy of thunderstorm forecasts from 1200 to 2100 by various factors were made in such a case. The results are shown in Table 1, where C is Slaven index; A is A index; K is K index; KYI is Koj Yamazat index (Koj Yamazat, 1975); LPI is lift parcel index; W_m is the max. vertical velocity computed in loaded moist adiabatic updraft model; E_{850}^{500} is instability energy released by air parcel which ascended from ground adiabatics when it passed through 850–500 hPa. It can be seen from the table that E_{850}^{500} is significantly superior to other stability factors.

Table 1 Comparison among Efficiencies of Various Stability Factors

Names of Factors	C	A	K	S	KYI	LPI	W_m	E_{850}^{500}
Critical Values	*−0.4°C*	*−14.8°C*	*27°C*	*−33°C*	*−0.4*	*1.4°C*	*11.3 m/s*	*267 J/kg*
Number of Hits	250	272	315	328	352	356	366	388
Accuracy (%)	40	44	51	53	57	57	59	62

Most of the stability factors currently used in operational work are computed based on sounding data. Because conventional upper air sounding network is established for synoptic scale system analysis, average spacing between stations is about 300–400 km; sounding time interval is 12 hours. Its temporal and spatial resolutions are inadequate for the analysis of severe convective storms whose life cycle spans for about several hours. Therefore, in very-short range weather forecast, analysis of hourly surface θ_e is frequently made to increase the temporal resolution. Recently, a high-resolution LPI distribution has been obtained by Hales with graphic subtraction (Hales and Doswell, 1982) and has been used as a tool for NSSFC (National Severe Storm Forecast Center) very short range forecast, the result of which is fairly good. In consideration that the E in forecasting severe convective storms is superior to LPI, and in order to meet the requirements for issue timing of very short range forecast, a high-resolution analysis method of instability energy was developed in this paper on the basis of a new method for computing instability energy (Li Hongji, 1985). Computation and analysis are done completely by computer and isogram of horizontal distributions of instability energy E can be obtained 20 seconds after data input. Tests have shown that the high-resolution analysis of instability energy is very useful to very short range forecast of severe convective storms.

II. THE GEOPOTENTIAL THICKNESS DIFFERENCE METHOD FOR COMPUTING INSTABILITY ENERGY

Since it is inconvenient to compute E with Eq. (1), this equation is rewritten as

$$E_{p_1}^{p_2} = g_0(\Delta H_{s\,p_1}^{p_2} - \Delta H_{p_1}^{p_2}) \tag{2}$$

where

$$g_0 = 9.80665 \text{ J/kg/gpm};$$

$$\Delta H_{p_1}^{p_2} = -\frac{R_d}{g_0}\int_{p_1}^{p_2} T_{vr} d\ln p = H_{p_2} - H_{p_1},$$

namely, the thickness of p_1–p_2 level can be estimated with geopotential height H_{p_1} and H_{p_2} of pressure levels p_1 and p_2 in sounding report, without the need of complete sounding curves.

$$\Delta H_{s\,p_1}^{p_2} = -\frac{R_d}{g_0}\int_{p_1}^{p_2} T_{vl} d\ln p \tag{3}$$

Assuming that virtual temperature distribution in air column is the same as the change in virtual temperature of adiabatic ascending parcel with altitude, $\Delta H_{s_{p_1}}^{p_2}$ is the thickness of "the adiabatic air column" between p_1 and p_2 (see Fig. 1), which is called adiabatic geopotential thickness. In Eq. (2) instability energy is considered as geopotential thickness difference between "adiabatic air column" from p_1 to p_2 and actual air column. It is physically understood as potential energy difference between unit mass air on top of the two air columns when air column bottoms are the same. We refer to the method for computing E with Eq. (2) as geopotential thickness difference method.

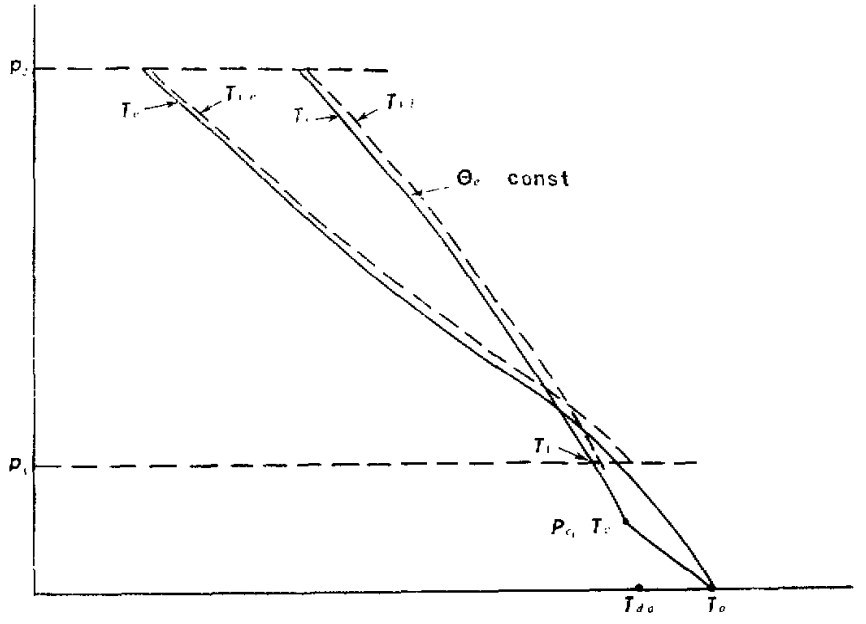

Fig. 1. Schematic diagram of the computation of the instability energy.

To compute E with (2), it is necessary to compute $\Delta H_{s_{p_1}}^{p_2}$. It can be seen from (3) that $\Delta H_{s_{p_1}}^{p_2}$ is a function of T_{vi} when p_1 and p_2 are constants. T_{vi} can be determined with adiabatic process. Considering the large diurnal variation of temperature stratification within boundary layer and under the disturbance, we should analyze the magnitude of E above the condensation level for forecasting severe convective storms. When determining the condensation level, altitude correction should be made first to derive the station pressure P because the surface pressure in weather report is usually the sea level pressure P_0 and it is not at the same altitude as the surface temperature T and the dew point temperature T_d (Central Bureau of Meteorology, 1954).

$$P = P_0 \times 10^{-\frac{h}{18400 \times \left(1 + \frac{T}{273}\right)}} \tag{4}$$

where h is the elevation of stations. Then, we may derive temperature T_c and pressure P_c at the condensation level using the following expression (Li Hongji, 1985):

$$T_c = T - \frac{T - T_d}{\gamma_d - 8.33 \times 10^{-4} \times \frac{(T_d - 35.9)^2}{Td}} \gamma_d$$

$$P_c = P\left(\frac{T_c}{T}\right)^{c_{pd}/R_d} \tag{5}$$

Thus, the equivalent potential temperature of surface parcel θ_e:

$$\theta_e = T_c\left(\frac{1000}{p_c - e_c}\right)^{R_d/c_{pd}} \cdot e^{\frac{L_c \omega_c}{c_{pd} T_c}} \tag{6}$$

where e_c and L_c are the saturation vapour pressure at the condensation level and the condensation latent heat of vapour, respectively, and they are the function of T_c; ω_c is the mixing ratio at condensation level; c_{pd} is the specific heat at constant pressure of dry air.

Above the condensation level, with $T_{vi} = T_i + \Delta T_{vi}$, the temperature of parcel taking adiabatic ascent T_i may be determined by following pseudo-adiabatic equation:

$$\ln T_i - \frac{R_d}{c_{pd}} \ln(p - e) + \frac{l\omega}{c_{pd} T_i} = \text{const} \tag{7}$$

namely, θ_e is constant. Virtual temperature correction ΔT_{vi} is calculated by the following equation:

$$\Delta T_{vi} = 0.378 \frac{e}{p} T_i \tag{8}$$

As shown in Fig. 1, with the given initial temperature T_1 for P_1 level above the condensation level, T_i can be computed level by level at an interval of 10 hPa by approximation method according to Eq. (7). After virtual temperature correction in (8), substituting it into (3), $\Delta H_{s_{P_1}}^{P_2}$ is obtained by using numerical integral. Thus, when P_1 and P_2 are constants, $\Delta H_{s_{P_1}}^{P_2}$ is only a function of θ_e.

What is the reliability of computation of E with (2)? A verification has been made by using 620 sounding data for July and August from 1969 to 1978 in Beijing. Every E_{800}^{500} value E_c is strictly computed by computer according to (1) and the corresponding E_{800}^{500} value E_t is computed according to (2), their correlation coefficient $r_{E_c E_t}$ being 0.98496. It can be seen that the geopotential thickness difference method for computing instability energy is reliable.

For convenience of manual calculation, we have made a table of $\Delta H_{s_{P_1}}^{P_2}$ values (Li Hongji, 1985).

III. COMPUTING METHOD OF HIGH-RESOLUTION INSTABILITY ENERGY

Observations have shown that the horizontal changes of weather elements within the boundary layer are often significant due to the influence of the underlying surface and, by compari-

son, that the changes within the mid-and-upper layer of troposphere are much milder. According to the geopotential thickness difference method of computing instability energy, $\Delta H_{s_{p_1}}^{p_2}$ is computed by using ground station network with comparatively dense horizontal distribution. The thickness over the ground stations is computed with the thickness of conventional upper air sounding stations near the region by using quadratic surface fitting. Thus, the distribution of high-resolution instability energy for ground station spacing is obtained. Because ground observing data are updated hourly, analysis and computation are done every hour in situation of development of favourably severe convective storms; therefore, computation and isopleth analysis must be done by computer.

1. *Interpolating Polynomial of* $\Delta H_{s_{p_1}}^{p_2}$

In order to compute E with computer, interpolating polynomial of $\Delta H_{s_{p_1}}^{p_2}$ is used to replace the $\Delta H_{s_{p_1}}^{p_2}$ table. Assuming

$$\Delta H_{s_{p_1}}^{p_2}(\theta_e(P,T,T_d)) \approx A(\theta_e)_{p_1}^{p_2} = a_{0_{p_1}}^{p_2} + a_{1_{p_1}}^{p_2}\theta_e + \cdots + a_{n_{p_1}}^{p_2}\theta_e^n, \tag{9}$$

we attempted to use the second, the third, the fourth, the fifth and the sixth order polynomial approximation. The results indicated that good fitting can be obtained with the third-order polynomial when P_1 and P_2 are different in thickness. Table 2 gives coefficients of interpolating polynomials and the maximum error from 850 hPa to each standard level. We can produce interpolating polynomials of $\Delta H_{s_{p_1}}^{p_2}$ between different standard isobaric surfaces according to our needs as given in Table 2. For example, for a plateau area where condensation level is at about 700 hPa, when it is necessary to compute E_{700}^{300}, interpolating polynomial of $\Delta H_{s_{700}}^{300}$ can be obtained in operation by subtraction of corresponding coefficients of $\Delta H_{s_{850}}^{300}$ and $\Delta H_{s_{850}}^{700}$ in the table because $\Delta H_{s_{700}}^{300} = \Delta H_{s_{850}}^{300} - \Delta H_{s_{850}}^{700}$. One can see from Table 2 the polynomials of different levels so constructed and error $|E_{max}| \leqslant 2$ gpm, whose accuracy entirely meets the needs of diagnosing stability distribution.

Table 2. Coefficient and Max. Error 'E_{max}' of $\Delta H_{s_{p_1}}^{p_2}$. Interpolating Polynomial ($299°K \leqslant \theta_e \leqslant 386°K$)

P_1-P_2	a_0	a_1	a_2	a_3	$\lvert E_{max}\rvert$
850–200	−9194.219	103.5267	−0.1510178	5.797127×10^{-5}	0.91
850–250	−11637.42	122.6696	−0.2257353	1.375143×10^{-4}	1.07
850–300	−13447.89	137.3381	−0.2877511	2.073517×10^{-4}	0.88
850–400	−13199.47	133.4619	−0.3115755	2.515794×10^{-4}	0.27
850–500	−9626.729	99.50077	−0.2397042	1.995988×10^{-4}	0.30
850–700	−3040.097	33.60977	-8.203626×10^{-2}	6.934624×10^{-5}	0.18

2. *Computation of Thickness Field* $\Delta H_{p_1}^{p_2}(x,y)$

For an upper air thickness field of several hundred kilometers, its distribution is assumed

to be a certain curved surface and the thickness field can be obtained approximately by the curved surface fitting. The commonly used method is quadratic surface fitting. In this paper, actual thickness is replaced by fitting thickness $B(x,y)$ approximation.

$$\Delta H_{p_1}^{p_2}(x,y) \approx B(x,y)_{p_1}^{p_2} = b_0 + b_1 x + b_2 y + b_3 x^2 + b_4 xy + b_5 y^2 \tag{10}$$

where x,y are distance of observing stations to the origin of coordinates. The following equations can be obtained by using least square method:

$$b_0 \sum^n 1 + b_1 \sum^n x_i + b_2 \sum^n y_i + b_3 \sum^n x_i^2 + b_4 \sum^n x_i y_i + b_5 \sum^n y_i^2 = \sum^n \Delta H_i$$

$$b_0 \sum^n x_i + b_1 \sum^n x_i^2 + b_2 \sum^n x_i y_i + b_3 \sum^n x_i^3 + b_4 \sum^n x_i^2 y_i + b_5 \sum^n x_i y_i^2 = \sum^n \Delta H_i x_i$$

$$b_0 \sum^n y_i + b_1 \sum^n x_i y_i + b_2 \sum^n y_i^2 + b_3 \sum^n x_i^2 y_i + b_4 \sum^n x_i y_i^2 + b_5 \sum^n y_i^3 = \sum^n \Delta H_i y_i$$

$$b_0 \sum^n x_i^2 + b_1 \sum^n x_i^3 + b_2 \sum^n x_i^2 y_i + b_3 \sum^n x_i^4 + b_4 \sum^n x_i^3 y_i + b_5 \sum^n x_i^2 y_i^2 = \sum^n \Delta H_i x_i^2$$

$$b_0 \sum^n x_i y_i + b_1 \sum^n x_i^2 y_i + b_2 \sum^n x_i y_i^2 + b_3 \sum^n x_i^3 y_i + b_4 \sum^n x_i^2 y_i^2 + b_5 \sum^n x_i y_i^3 = \sum^n \Delta H_i x_i y_i$$

$$b_0 \sum^n y_i^2 + b_1 \sum^n x_i y_i^2 + b_2 \sum^n y_i^3 + b_3 \sum^n x_i^2 y_i^2 + b_4 \sum^n x_i y_i^3 + b_5 \sum^n y_i^4 = \sum^n \Delta H_i y_i^2$$

namely,

$$\begin{pmatrix} N & \Sigma x & \Sigma y & \Sigma x^2 & \Sigma xy & \Sigma y^2 \\ \Sigma x & \Sigma x^2 & \Sigma xy & \Sigma x^3 & \Sigma x^2 y & \Sigma xy^2 \\ \Sigma y & \Sigma xy & \Sigma y^2 & \Sigma x^2 y & \Sigma xy^2 & \Sigma y^3 \\ \Sigma x^2 & \Sigma x^3 & \Sigma x^2 y & \Sigma x^4 & \Sigma x^3 y & \Sigma x^2 y^2 \\ \Sigma xy & \Sigma x^2 y & \Sigma xy^2 & \Sigma x^3 y & \Sigma x^2 y^2 & \Sigma xy^3 \\ \Sigma y^2 & \Sigma xy^2 & \Sigma y^3 & \Sigma x^2 y^2 & \Sigma xy^3 & \Sigma y^4 \end{pmatrix} \begin{pmatrix} b_0 \\ b_1 \\ b_2 \\ b_3 \\ b_4 \\ b_5 \end{pmatrix} = \begin{pmatrix} \Sigma \Delta H \\ \Sigma \Delta H \cdot x \\ \Sigma \Delta H \cdot y \\ \Sigma \Delta H \cdot x^2 \\ \Sigma \Delta H \cdot xy \\ \Sigma \Delta H \cdot y^2 \end{pmatrix} \tag{11}$$

In the above-mentioned equations, $\sum^n$ is replaced by Σ, the subscripts of x_i and y_i, ΔH_i are omitted, and N is the number of upper air data.

The equation of the quadratic surface has 6 coefficients; therefore, data from over 6 stations are needed. Normally, the region of stations selected should be larger than the analysed one, and should be scattered around the region with 1 or 2 stations in the center. The thickness taken from soundings is substituted into (11) for the solution of $b_j\ (j=0,1,\ldots,5)$. Finally, they are substituted into (10) to obtain fitting thickness over ground stations according to coordinates x,y of ground stations.

When sounding data are less than 6 but more than 3, and analysis region is relatively small, a linear planar fitting can be made for the thickness over ground stations. Results similar to that of (11) can be obtained with the same method.

We verified quadratic surface fitting thickness by using the data from the sounding network of the Eastern China Mesoscale Experiment. Twenty or so sounding stations

were added to the area of 7 conventional sounding stations (Xuzhou, Sheyang, Fuyang, Nanjing, Anqing, Hangzhou, Shanghai) in East China, and the sounding data of 90 km in horizontal distance are available. There were altogether 29 sounding records in this region at 0800 May 30, 1982. The root-mean-square error for the 400-850 hPa thickness fitting value is 10.9 gpm. Twenty-four sounding records were obtained within the area at 0800 June 17, 1982, with root-mean-square error being 10.1 gpm. Such a difference was probably due to the fact that the comparatively dense sounding data reflected certain mesoscale disturbances.

Substituting (9) and (10) into (2), we have

$$E_{p_1}^{p_2} \approx g_0[A(\theta_e)_{p_1}^{p_2} - B(x,y)_{p_1}^{p_2}] \tag{12}$$

Figures 2 and 3 are the E_{850}^{700} distributions computed with denser-spacing sounding data for the

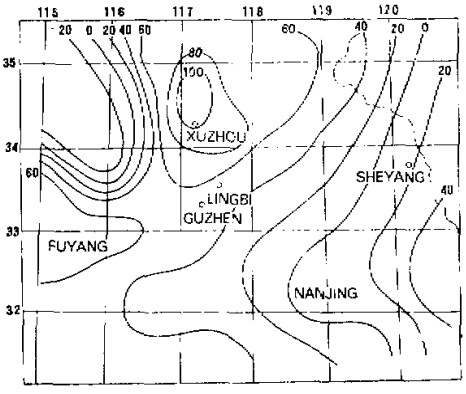

Fig. 2. The E distribution for 0800 June 17,1982 computed by denser sounding station. Unit: 9.8 J/kg (Thereafter).

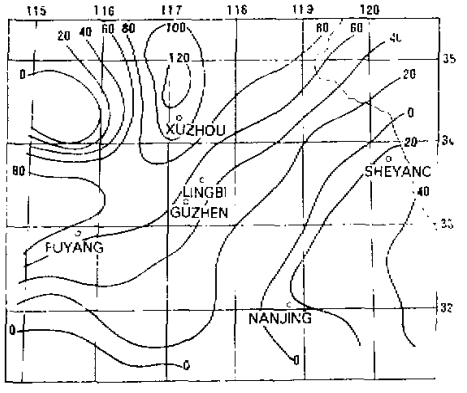

Fig.3. The E distribution for the same time as Fig.2 computed by fitting method.

experiment, and E_{850}^{700} distribution obtained from (12) based on data for the above-mentioned 7 conventional sounding stations at 0800 June 17, 1982, separately. It can be seen that the E distribution obtained by two methods are basically consistent in patterns, except for remote regions. Therefore, the high-resolution E analysis method is reliable.

Because METAR has surface data every hour while conventional upper air thickness data are obtained once every 12 hours, for thickness of non-sounding time, $B(x,y)$ can be translationally extrapolated. Let $X=x-u(t-t_0)$ and $Y=y-v(t-t_0)$,where u and v are the moving speed of thickness field. Generally, they can be given according to the moving speed of upper air trough or ridge at a forecast time. t_0 is the time for upper air sounding. Thus,

$$E_{p_1}^{p_2} \approx g_0[A(\theta_e, t)_{p_1}^{p_2} - B(x-u(t-t_0), y-v(t-t_0))_{p_1}^{p_2}]. \tag{13}$$

Horizontal distribution of hourly instability energy can be obtained according to (13). When weather situation is stable or $t-t_0$ is comparatively small, we can also simply assume that the change in thickness field is rather small within a short period of time (at least relative to the change in surface elements), and the thickness of corresponding time is replaced by that at 0800,

With the development of numerical weather prediction, we can also obtain thickness distribution several hours in advance using the result of numerical prediction.

IV. APPLICATION

A comparison is made between the high-resolution E analysis method and the method for computing E with only conventional sounding data, i.e. the low-resolution method. Figure 4 shows the low resolution E distribution for the eastern China at 0800 May 30, 1982. It can be seen from Fig. 4 that there is a wide E ridge stretching from SW to the lower reaches of Changjiang River. A 20×9.8 J/kg isopleth reaches as far as the area north of the Changjiang River. It seems that the areas in the middle and lower reaches are favourable to the occur rence of severe convective storms. As for the actual location of occurrence, it is difficult to judge. Figure 5 is the high-resolution E distribution for the same time as Fig. 4. It

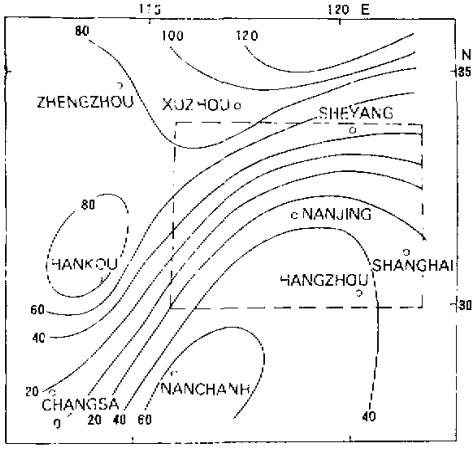

Fig. 4. Low-resolution E distribution at 0800 May 30, 1982.

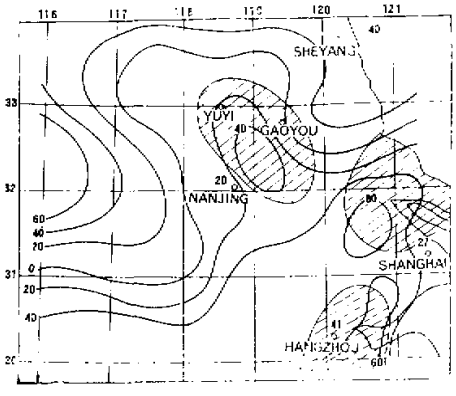

Fig. 5. High-resolution E distribution for the same time as Fig. 4. Shaded area is thunderstorm area at 1500.

corresponds to the area encircled by dotted line in Fig. 4. In this figure, E distribution presents an obvious Ω shape, and there are 3 areas of large E value, which are all higher than E values of the four conventional sounding stations (Nanjing, Sheyang, Shanghai and Hangzhou) in the region. The distribution of such mesoscale instability energy is smoothed in Fig. 4. In fact, thunderstorms occurred along Yuyi, Gaoyou and Hangzhou Bay from 1100 am that day. In Fig. 5 the two areas of large E value in the north corresponds to the two active thunderstorm areas: hail and gale occurred in a large E area near Hangzhou Bay in the south. High-resolution E distribution at 0800 that day corresponds to the severe convective storm activity 12 hours later quite well. For very short range forecast of severe convective storms, it is more effective than the low resolution analysis.

The analysis method of high-resolution instability energy has not only improved the spatial resolution of stability analysis, but also raised its temporal resolution. As shown in Fig. 2, there was a large E value near Xuzhou at 0800 June 17, 1982. Thunderstorms occurred

in northern Xuzhou first in the afternoon. By about 1740 the thunderstorm area had moved near Lingbi and Guzhen, thunderstorms strongly developed, and hail and gale of 35 m/s occurred. Figure 6 shows the instability energy distribution at 1700 obtained by using high-resolution E computing method. The center of E was moving near Lingbi, consistent very well with the area of severe storms half an hour later. The magnitude of positive value center and that of horizontal gradient of E are closely correlated with the strength change and moving direction of thunderstorms in a short period.

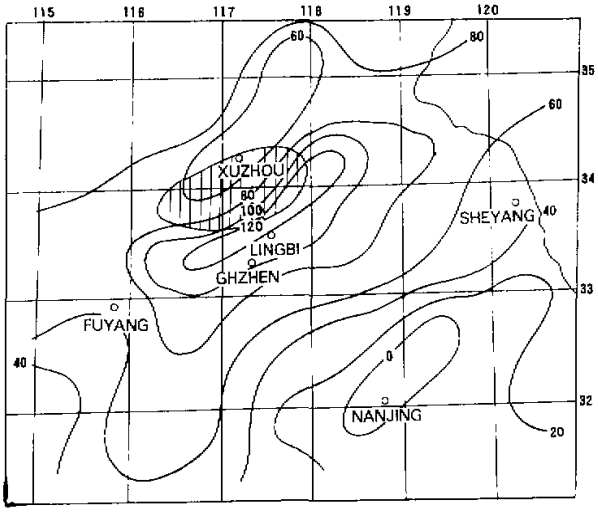

Fig. 6. Distribution of E and thunderstorm at 1700 June 17,1982.

From June to August 1985, the high-resolution analysis method of E was used in Nanjing. Surface data used were METAR, which were obtained once an hour for the Nanjing Military Area. The average distance among 51 ground stations was about 60 km. The thickness of 850–300 hPa was obtained from conventional sounding data of about 10 stations in and around the Military Area. The horizontal distributions of E_{850}^{300} divergence, flow field, θ_e, etc. can be obtained in graphic form 20 seconds after data input. In the operational work, computation is done at 1000 every day. In case there exists a condition favourable to the occurrence of severe convective storms or when a thunderstorm has already occurred, the number of computation would be increased. Computation is done at 1000 am becuase the 850 hPa and 300 hPa upper air data for 0800 can be received at about 1030, when inversion near the surface had basically disappeared by then, and computational results are representative. It was seen from the tests that the distribution chart of E at 1000 was a good indication of severe convective storm activities in the afternoon and at dusk. For example, in the high-resolution distribution chart of E at 1000 June 24 (Fig. 7), there was a region of positive value exceeding 100×9.8 J/kg in the south, while in the north, the E isopleth was very tight. A strong convective storm occurred just near the large value region in the afternoon. This process occurred somewhere among the three sounding stations of Anqing, Hangzhou and Juxian. Obviously, it is difficult to forecast this severe convective storm only with data of the above-mentioned sounding stations. It can be seen that a high-resolution analysis of E can

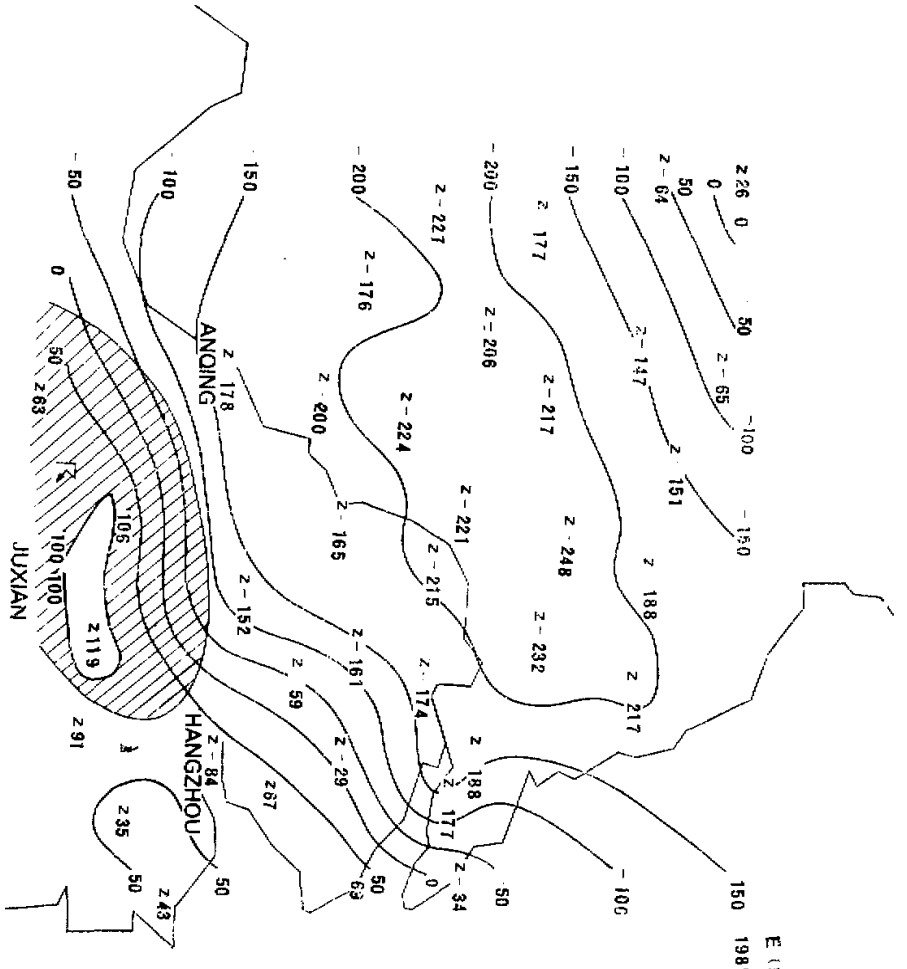

Fig. 7. Distribution of E at 1000 am June 24, 1985 and thunderstorm area in the afternoon.

show mesoscale characteristics of E and provide valuable information for severe convective storm forecast. Therefore, it is a useful tool.

The horizontal distribution of E directly reflects the buoyancy instability in the region, and it is also related to baroclinic instability. The occurrence and development of severe convective storms are also closely correlated with the disturbance of flow field in the boundary layer. An analysis of Nanjing Area shows that the vorticity of surface wind is less correlated with severe convective storm activities. The combination of high-resolution horizontal distribution of E and surface divergence gives better results. The matching areas of positive value center of E over 40×9.8 J/kg at 1000 with its convergence center below $-10^{-4}s^{-1}$ in the surface observing network are usually those regions where the afternoon thunderstorm often occurs. Normally, thunderstorm moves to the positive value center of E and to the convergence center. When both gradients of E and convergence are relatively large in the direction of thunderstorm movement, the thunderstorm will obviously be intensified in a short span of time.

V. CONCLUSION

Observations show that the air involved in cumulus convection comes mainly from the lower layer of atmosphere. The magnitude of instability energy released by low-level air during its ascent has significant influence on the occurrence and development of severe convective storms. Within the boundary layer, horizontal distribution of atmosphere state is rather nonuniform and dinural change is very great, which are important for the activity of severe convective storms. Based on this understanding, the geopotential thickness difference method for computing instability energy and the high-resolution analysis method of instability energy were suggested in this paper. These computating methods not only facilitate the computation of E in operational work, but also significantly increase its temporal and spatial resolution. The horizontal distribution chart of E with high resolution and surface divergence field may explain some phenomena in the occurrence, development and movement of severe convective storms, and they are useful to the analysis and forecast of heavy rain and severe convective storms.

REFERENCES

Central Bureau of Meteorology (1954), Meteorological Table in common use (in Chinese), No. 3.

Chao Jiping and Zhou Xiaoping (1964), Dynamics of cumulus (in Chinese), Scientific Publishing House.

Chisholm, A.J. (1973), Alberta hailstorms, AMS.

Hales, J.E. and C.A. Doswell (1982), High resolution diagnosis of instability using hourly surface lift parcel temperature, Preprints, 12th Conference on Severe Local Storms.

Koj Yamazat (1975), Three conditions of convection and K.Y. index—A method of heavy rain forecast (in Japanese), Journal of Meteorological Research, No. 27, 347-352.

Li Hongji (1985), A new method of computing instability energy and its application (in Chinese with English abstract), Acta Meteorologica Sinica, 43: No. 1, 63-71.